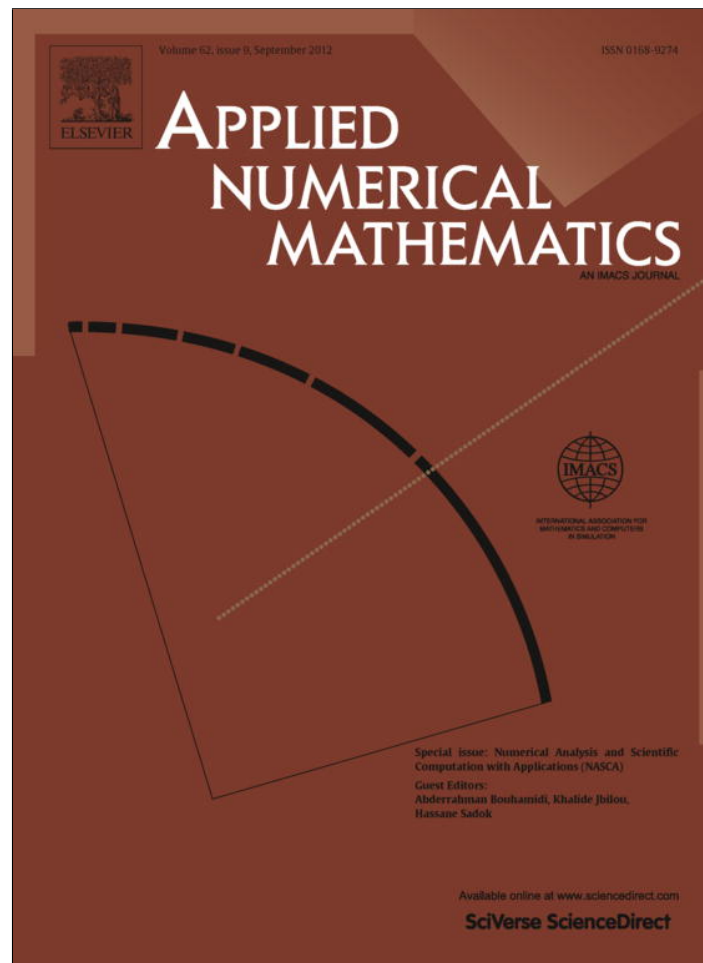


Provided for non-commercial research and education use.
Not for reproduction, distribution or commercial use.



This article appeared in a journal published by Elsevier. The attached copy is furnished to the author for internal non-commercial research and education use, including for instruction at the authors institution and sharing with colleagues.

Other uses, including reproduction and distribution, or selling or licensing copies, or posting to personal, institutional or third party websites are prohibited.

In most cases authors are permitted to post their version of the article (e.g. in Word or Tex form) to their personal website or institutional repository. Authors requiring further information regarding Elsevier's archiving and manuscript policies are encouraged to visit:

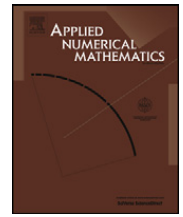
<http://www.elsevier.com/copyright>



Contents lists available at [SciVerse ScienceDirect](http://SciVerse.ScienceDirect.com)

Applied Numerical Mathematics

www.elsevier.com/locate/apnum



Heat transfer modeling in saturated porous media and identification of the thermophysical properties of the soil by inverse problem

Mohamad Muhieddine^{a,*}, Édouard Canot^b, Ramiro March^c

^a LIU, Beirut, Lebanon

^b IRISA, Campus de Beaulieu, Rennes, France

^c CReAAH, Campus de Beaulieu, Rennes, France

ARTICLE INFO

Article history:

Available online 15 May 2012

Keywords:

Inverse problem
Heat transfer
Phase change
Algebraic system
Gauss–Newton method

ABSTRACT

In this paper, the authors introduce a robust numerical strategy to estimate the temperature dependent heat capacity, thermal conductivity and porosity of a saturated porous medium, basing on the knowledge of heating curves at selected points in the medium. In order to solve the inverse problem, we use the least squares criterion (in which the sensitivity coefficients appear), leading to a system of ordinary differential equations (ODE). At the stage of numerical computations, we propose a new global approach, based on the method of lines and ordinary differential equations solvers, combined with a modified Newton method to deal with the nonlinearities presented in the system of coupled equations.

© 2012 IMACS. Published by Elsevier B.V. All rights reserved.

1. Introduction

This work is motivated by the studies of archaeological soils. The purpose is to present a systematic application of numerical modeling and replication experiments in a particular field of archaeological research which is the study of archaeological hearths, used for cooking and heating by ancient human groups. It is usually accepted that the utilization of energy and the control of its related maximal temperature, implied in different activities like cooking, baking, pottery fabrication and the elaboration of metals and non-metals by ancient civilizations, may help in their characterization. The idea is to apply a numerical model to calculate the unsteady heat conduction in water saturated porous soils subjected to intense heating from above. In the early applications it seemed that it was not necessary to consider the effects of humidity [18]. It was so because soils made from mussel's shells were sufficiently "ventilated". In this case it was only necessary to simulate the equivalent dry soil properties, under the rather restrictive hypothesis of no air movement. When attention was focused on argillaceous soils like those at Pincevent or Etiolles, there were need to consider the effect of water content [6].

The evaporation of water in the porous soil (due to the phase change phenomenon) must be taken into consideration when dealing with humid soil. This problem is classified as a moving boundary problem which has been of special interest due to the inherent difficulties associated with the nonlinearity of the interface conditions and the unknown locations of the moving boundaries. In this respect, the "apparent heat capacity method" [17] (otherwise called "effective heat capacity method") was adopted to calculate the adequate values for the equivalent thermodynamic properties of the soil and this approach will be the subject for further discussion in the following sections. Firstly, if the parameters appearing in the governing equations are known then the forward problem is considered. This problem, which reproduces the experimental thermal behavior for dry and wet sedimentaries, has been solved by the authors in 1, 2 and 3 dimensions [18,16]. However, if part of these parameters is unknown then the inverse problem should be formulated.

* Corresponding author.

E-mail addresses: mohamad.muhieddine@liu.edu.lb (M. Muhieddine), edouard.canot@irisa.fr (É. Canot), ramiro.march@univ-rennes1.fr (R. March).

Actually, two types of inverse heat conduction problems are mainly identified: the first one contains boundary heat flux reconstruction and heat source identification, while the other one is the thermal properties estimation on which we focus our study in this paper.

Our problem of interest in this paper is the inverse problem consisting in the estimation of thermophysical parameters of the soil. On the basis of the knowledge of heating curves at selected points from the altered soil (called observations), the thermal conductivity, the volumetric heat capacity and the porosity of the soil are simultaneously identified. However, many possible difficulties appear:

- First of all is how to obtain the observations: an experiment is never easy to realize! Indeed, in our case, it is not realistic to suppose that we can measure the temperature at each point of the computational domain and then we cannot have sufficient number of observations compared to the number of unknown parameters.
- In addition, it is obvious that if the temperature is constant in a sub-domain of the soil, the conductivity could not be determined. To fill this lack, we should have more informations.
- Also, there is no exact measure, and the mathematical model of the forward problem does not reflect the exact reality. Thus, there is, in fact, no reason that the inverse problem has a solution.
- Finally, because of the complexity of certain real systems and because of the lack of data, the inverse problem is often an “ill-posed problem” in the meaning of Hadamard [7]. This means that the problem satisfies one of the in-existence conditions, the non-unicity or the instability of the solution. This limits usually the use of inverse problem and makes impossible the resolution of the problem. In addition, we can talk about the nonsensibility of the model when the observations do not contain sufficient informations to insure the estimation of parameters.

The resolution of inverse problem requires a good knowledge of the forward problem, that means it requires the need of large variety of as well as physical as mathematical concepts. Thus, many numerical techniques have been proposed to solve such problems, mainly two approaches are used in the literature: the regularization of ill-posed problem and the least squares formulation.

The reformulation of the inverse problem as the minimization of an error function between the real measures and the synthetic ones (which are the solution of the forward problem) is the most important technique used to solve such a problem. It will be convenient to distinguish between the linear and the nonlinear problems. We have to state that the nonlinearity we are talking here is the one presented in the inverse problem and not that of the forward problem.

When dealing with linear problems [9], the use of the linear algebra and the functional analysis allows us to obtain precise results and to find efficient algorithms. The fundamental tool here is the singular value decomposition (SVD) of the considered operator.

Otherwise, the nonlinear problems are more difficult [10], and there is less general results. The nonlinear methods use an iterative procedure to optimize the parameters: the resolution of the diffusion equation, the verification of the adjustment between the calculated temperature and the observed one and the modification of the parameters in order to improve the adjustment are repeated till the difference between the measured temperatures and the calculated ones reaches a minimum (often the order of magnitude for the measure errors in temperatures).

Many methods have been proposed to solve inverse heat transfer problems, like Levenberg–Marquardt method presented by Mejias and Orlande [14] to examine the inverse problem concerning the identification of the three thermal conductivity components of an orthotropic cube. Also, four different versions of the conjugate gradient method are presented by these authors.

The Bayesian approach has been proposed by Wang and Zabarar [21] for the solution of the inverse heat conduction problem. In this work, the posterior probabilistic density function of the boundary heat flux has been computed given temperature measurements within a conducting solid.

An integral approach has been developed in [8] to estimate temperature dependent thermal conductivity without internal measurements. Authors claimed that the proposed approach may be useful to make sufficiently accurate the initial guess for the inverse heat conduction problem in order to determine the thermal conductivity having an arbitrary function form.

In [11–13], authors discussed the problem of identification of physical, boundary and initial conditions determining the mathematical description of casting solidification. The identification algorithms described by the authors are based on the least squares criterion.

In this paper, we used the least squares criterion in which the sensitivity coefficients appear [1], in order to solve the inverse problem. In order to determine these sensitivity coefficients, three additional boundary initial problems resulting from the differentiation of basic equations with respect to the thermal parameters of the soil must be solved. On the stage of numerical computations, the spatial discretization of the system is obtained by using the vertex-centered finite volume method. The discretized problem to be solved may be written in vectorial form with adequate initial and boundary conditions using the method of lines where space and time discretizations are considered separately, leading to a semi-discrete system of implicit differential equations. The time integration method is performed by the `DASSL` solver [3] which has been used to achieve stability and the prescribed accuracy by adjusting automatically the time step in a fixed-leading-coefficient form. The code validation stage is based on the comparison between the numerical results and synthetic data; this comparison shows a good agreement.

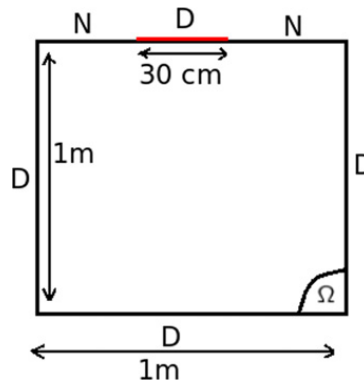


Fig. 1. The computational domain. N: Neumann condition, D: Dirichlet condition.

2. Forward problem governing equations

Our problem of heat diffusion in a saturated porous media is characterized by solving the partial differential equation obtained by combining Fourier’s law of heat conduction and the law of conservation of energy. The parabolic governing equation for the unknown T is given by

$$\begin{aligned}
 (\rho C)_e(T) \frac{\partial T(x, t)}{\partial t} + \nabla q &= 0 \quad \text{in } \Omega \times (0, t_{end}] \\
 q &= -k(T) \nabla T(x, t) \quad \text{in } \Omega \times (0, t_{end}] \\
 T(x, 0) &= T_0(x) \quad \text{in } \Omega \\
 T(x, t) &= T^D(x, t) \quad \text{on } \Gamma^D \times (0, t_{end}] \\
 T(x, t) \cdot \nu &= q^N(x, t) \quad \text{on } \Gamma^N \times (0, t_{end}]
 \end{aligned}
 \tag{1}$$

where Ω is a bounded domain in \mathbb{R}^d ($d = 1, \dots, 3$) with boundary $\partial\Omega = \Gamma^D \cup \Gamma^N$ (see Fig. 1); $(\rho C)_e = \phi(\rho C)_f + (1 - \phi)(\rho C)_s$ (where $(\rho C)_f = \rho_f C_f$ and $(\rho C)_s = \rho_s C_s$) represents the effective volumetric heat capacity of the medium (ρ is the density, C is the specific heat capacity, ϕ is the porosity, the subscripts e, f and s indicate respectively the equivalent parameters of the medium, the properties of the fluid and the porous matrix properties); k_e is the conductivity, it is assumed to be a diagonal tensor with components in $L^\infty(\Omega)$ (k_e is calculated using the harmonic mean between k_f and k_s); ν indicates the outward unit normal vector along $\partial\Omega$; T^D and q^N are respectively the Dirichlet and Neumann boundary conditions. The form of the system (1) shows that only conduction heat transfer is considered and that the convection in the phase change sub-domain is neglected. It should be mentioned that the thermophysical properties of the fluid are temperature dependent and that is why the problem is highly nonlinear.

When a heated region in the soil reaches T_{sat} (temperature of saturation which is approximately 100°C), the water existing in the soil turns into gas flowing in the ground. Our problem is then a dry/wet phase change problem (moving boundary problem), and to avoid the tracking of the dry/wet interface, the apparent heat capacity method will be used [2,15]. In this method, the latent heat is taken into consideration by integrating the specific heat capacity over the temperature, and the computational domain is considered as one region. As the relationship between specific heat capacity and temperature in isothermal problems involves sudden changes, the zero-width phase change interval must be approximated by a narrow range of phase change temperatures. Thus, the size of time steps must be small enough so that this temperature range is not overlooked in the calculation. According to [2], if the physical properties do not depend on temperature (i.e. when k_l, C_l, k_v and C_v are constants), the equivalent parameters may be obtained taking into consideration that the phase change takes place in a small temperature interval ΔT (see Fig. 2), but we don’t see any explanation for this limitation; practically we use the same method even if all coefficients are temperature dependent.

$$C_f = \begin{cases} C_l, & T < T_v - \frac{\Delta T}{2} \\ \frac{C_v + C_l}{2} + \frac{L}{\rho \Delta T}, & T_v - \frac{\Delta T}{2} \leq T \leq T_v + \frac{\Delta T}{2} \\ C_v, & T > T_v + \frac{\Delta T}{2} \end{cases}
 \tag{2}$$

where L is the latent heat of phase change, T_v is the phase change temperature. Similarly a global new thermal conductivity must be introduced:

$$k_f = \begin{cases} k_l, & T < T_v - \frac{\Delta T}{2} \\ k_l + \frac{k_v - k_l}{\Delta T} [T - (T_v - \frac{\Delta T}{2})], & T_v - \frac{\Delta T}{2} \leq T \leq T_v + \frac{\Delta T}{2} \\ k_v, & T > T_v + \frac{\Delta T}{2} \end{cases}
 \tag{3}$$

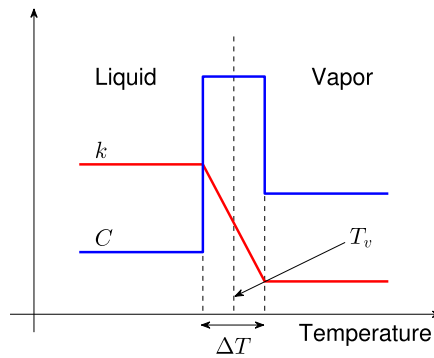


Fig. 2. Physical properties given by Bonacina.

However, the apparent heat capacity (AHC) formulation suffers from a singularity problem for the physical properties C (specific heat capacity) and k (thermal conductivity) (see Fig. 2). Thus, in the following we propose a new formulation of the physical parameters of the fluid to avoid this problem.

The numerical solution can be obtained as the limit of a uniformly convergent sequence of classical solutions to the approximated problems, deduced by smoothing the coefficients (2), (3), following a few general rules [4]: the apparent heat capacity formulation allows for a continuous treatment of a system involving phase transfer. If the phase transition takes place instantaneously at a fixed temperature, then a mathematical function such as

$$\sigma = \chi(T - T_v) \tag{4}$$

is representative of the volumetric fraction of the initial phase (liquid phase). χ is a step function whose value is zero when $T < T_v$ and one otherwise. Its derivative, i.e., the variation of the initial phase fraction with temperature, is

$$\frac{d\sigma}{dT} = \delta(T - T_v) \tag{5}$$

in which $\delta(T - T_v)$ is the Dirac delta function whose value is infinity at the transition temperature, T_v , and zero at all other temperatures. To alleviate the present singularity the Dirac delta function can be approximated by the normal distribution function

$$\frac{d\sigma}{dT} = (\epsilon\pi^{-1/2}) \exp[-\epsilon^2(T - T_v)^2] \tag{6}$$

in which ϵ is chosen to be $\epsilon = \sqrt{2}/\Delta T$ and where ΔT is the assumed phase change interval. Consequently, the integral of Eq. (6) yields the error functions approximations for the initial phase fraction

$$\sigma(T) = \frac{1}{2}(1 + \text{erf}(\epsilon(T - T_v))) \tag{7}$$

With conventional finite volume method, the initial phase fraction derived from Eq. (6) by integration should be used to avoid the numerical instabilities arising from the jump in the values of the volumetric fraction of initial phase from zero to one.

In our approach we assume for simplicity that the phases are isotropic and homogeneous. Accordingly, the smoothed coefficients (see Fig. 3) of Eqs. (2) and (3) could be written as:

$$C_f = C_l + (C_v - C_l)\sigma + L\frac{d\sigma}{dT} \tag{8}$$

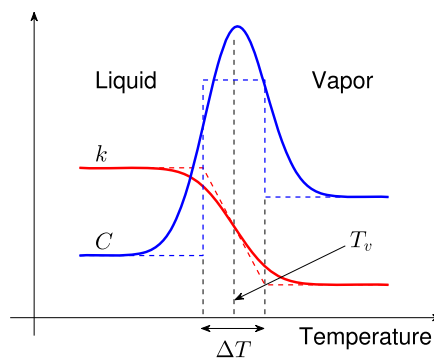


Fig. 3. Smoothed physical properties used by our model.

and

$$k_f = k_l + (k_v - k_l)\sigma \tag{9}$$

To avoid the resolution of the problem in two different regions, we generalized this approximation for the density which is formulated by:

$$\rho_f = \rho_l + (\rho_v - \rho_l)\sigma \tag{10}$$

where ρ_l and ρ_v remain constants.

3. Inverse problem

As we mentioned in the introduction, our problem of interest is to estimate the volumetric heat capacity $(\rho C)_s$, the conductivity k_s and the porosity ϕ of saturated soils by inverse problem. However, to give a theoretical formulation of the problem which we consider thereafter, we introduce three fundamental spaces with finite dimensions (we suppose that we discretized the problem in time and space):

- R the space of unknown parameters $((\rho C)_s, k_s, \phi)$, with dimension $P = 3$;
- U the state space, with dimension M ;
- D the space of data (or observations), with dimension N .

First of all, we are going to define the state equation which links implicitly the parameter to the state variable (temperature) (obviously, both could be vectors). We write:

$$F(p, T) = 0, \quad p = (p_j)_{1 \leq j \leq P} \in R \text{ and } T = (T_i)_{1 \leq i \leq M} \in U \tag{11}$$

whose solution is T_p , then we define the observation equation which extracts from the state variable the part corresponding to the measurements. The inverse problem consists then, given an observation T_g , in solving the equation:

$$g(p) = T_g \tag{12}$$

The application g is nonlinear, that makes obviously more difficult the resolution of the inverse problem. We are going to introduce a priori weaker formulation, which is very useful. We replace Eq. (12) by the following minimization problem,

$$\text{minimize } S(p) = \frac{1}{2} \|g(p) - T_g\|_2^2 \tag{13}$$

This is the least squares method, and S is the cost function or error function. Once we have the observation, in order to evaluate the functional S on parameter p , we start by solving the state equation (11), then we calculate $g(p)$ and we compare the simulated observation versus the measured one. We suppose that solving (13) is a good approximation for the continuous problem.

Thus, in order to solve our problem, the least squares criterion is applied and the inverse problem is formulated as follows

$$\text{minimize } S((\rho C)_s, k_s, \phi) = \frac{1}{MF} \sum_{f=1}^F \sum_{i=1}^M (T_i^f - T_{gi}^f)^2 \tag{14}$$

where $T_i^f = T(x_i, t_f)$ are the temperatures being the solution of the forward problem for the assumed set of parameters at the points $x_i, i = 1, 2, \dots, M$ for the time $t_f, f = 1, 2, \dots, F$, and T_{gi}^f are the measured temperatures at the same points x_i for time t_f . Thus, $N = MF$ is the dimension of the data space D . S is the cost function or the error function.

Usually, in literature the use of the Tikhonov regularization is more preferred than the least squares criterion but in our case the use of this last is justified by the small number of unknown parameters in comparison to the number of observation data. Actually, the calculation of the conditioning of the Jacobian matrix shows that the matrix is not too bad (10^3 till 10^4).

3.1. Difficulties and proposed algorithms

Many difficulties arise in the resolution of inverse problem:

- The cost function S is nonconvex. This lead to the existence of local minimum in the solutions, in other words several parameters may produce the same observations.
- The lack of continuity gives an instability. Even if we can (in theory) solve the problem for exact observations, it doesn't mean that we can solve it for disturbed data.

- Another difficulty is related to the cost of resolution. In fact, the simple resolution of the cost function S requires the resolution of state equation, that means in general the resolution of one or many partial differential equations.

To solve the least squares problem (14), two proposed algorithms are usually used in the literature [20]:

- The local algorithms which exploit the given information by the gradient of the functional S to be minimized and seek to solve an equation provided by an optimality condition of first order. The principal disadvantage of these algorithms is that it could converge toward a local minimum, or a critical point. Therefore, we have to use the second derivative to drive away the critical points which are not minima.
- Local algorithms face the methods known as global algorithms which exploit the space of parameters to converge toward the global minimum. These methods have sometimes an heuristic aspect and are basically more expensive and slower than the local algorithms. However, these methods have the advantage to avoid the calculation of the gradient for the cost function, which is usually a difficult point.

3.2. Resolution by Gauss–Newton method

Let us define the following vectors

$$T_g = \begin{pmatrix} T_{g1}^1 \\ \dots \\ T_{g1}^F \\ T_{g2}^1 \\ \dots \\ T_{g2}^F \\ \dots \\ T_{gM}^1 \\ \dots \\ T_{gM}^F \end{pmatrix}, \quad g(p^{(k)}) = \begin{pmatrix} T_1^{1,(k)} \\ \dots \\ T_1^{F,(k)} \\ T_2^{1,(k)} \\ \dots \\ T_2^{F,(k)} \\ \dots \\ T_M^{1,(k)} \\ \dots \\ T_M^{F,(k)} \end{pmatrix}, \quad p^{(k)} = \begin{pmatrix} (\rho C)_s^{(k)} \\ K_s^{(k)} \\ \phi_s^{(k)} \end{pmatrix}$$

and

$$r(p^{(k)}) = g(p^{(k)}) - T_g$$

represents the error in the model prediction at the iteration k .

The basic methods for the nonlinear least squares problem (14) require derivative informations about the components of $r(p^{(k)})$. The Jacobian of the residual vector $r(p^{(k)}) = (r_i(p^{(k)}))_{1 \leq i \leq N}$ is

$$J(p^{(k)}) \in \mathbb{R}^{N \times P}, \quad J(p^{(k)})_{i,j} = \frac{\partial r_i(p^{(k)})}{\partial p_j^{(k)}} \tag{15}$$

$i = 1, \dots, N, j = 1, \dots, P$.

Then the first derivative of $S(p^{(k)}) = \frac{1}{2} r(p^{(k)})^t r(p^{(k)})$ is given by:

$$\nabla S(p^{(k)}) = J(p^{(k)})^t r(p^{(k)}) \tag{16}$$

A necessary condition for p^* to be a local minimum of $S(p^{(k)})$ is that

$$\nabla S(p^*) = J(p^*) r(p^*) = 0 \tag{17}$$

Any point which satisfies this condition will be called a critical point (see Fig. 4). We should mention that this condition is not a necessary one for a critical point p^* to be a local minimum of $S(p^{(k)})$.

The special form of $S(p^{(k)})$ can be exploited by different methods for the nonlinear least squares problem, we choose to use the Gauss–Newton method which has the advantage to solve the problem (14) by a small number of iterations and to converge quickly toward the local solution p^* such as $J(p^*) r(p^*) = 0$. The Gauss–Newton method for the problem (14) is based on a sequence of linear approximations of $r(p^{(k)})$:

$$\tilde{r}(p^{(k)}) = r(p^{(k)}) + J(p^{(k)})(p - p^{(k)}) \tag{18}$$

Now, to calculate the approximated solution of (14) we can use the linearized least squares problem:

$$\min_m \|r(p^{(k)}) + J(p^{(k)})m\|_2 \tag{19}$$

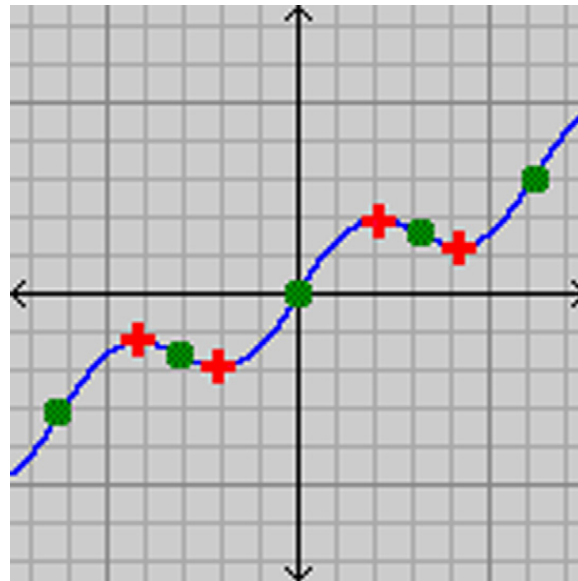


Fig. 4. Stationary points (red pluses) and inflection points (green circles). It's important to note that the stationary points are critical points, but the inflection points are not.

By using the Gauss–Newton method, if $p^{(k)}$ is the current approximation, the correction $m^{(k)}$ is calculated as the solution of the linear least squares problem (19) and the new approximation is written as follows:

$$p^{(k+1)} = p^{(k)} + m^{(k)} \tag{20}$$

This linear least squares problem is solved using QR decomposition of $J(p^{(k)})$ obtained by differentiating explicitly the state equation with respect to the unknown parameters

$$J(p^{(k)}) = \frac{2}{MF} \begin{pmatrix} W_1^{1,(k)} & R_1^{1,(k)} & Z_1^{1,(k)} \\ \dots & \dots & \dots \\ W_1^{F,(k)} & R_1^{F,(k)} & Z_1^{F,(k)} \\ W_2^{1,(k)} & R_2^{1,(k)} & Z_2^{1,(k)} \\ \dots & \dots & \dots \\ W_2^{F,(k)} & R_2^{F,(k)} & Z_2^{F,(k)} \\ \dots & \dots & \dots \\ W_M^{1,(k)} & R_M^{1,(k)} & Z_M^{1,(k)} \\ \dots & \dots & \dots \\ W_M^{F,(k)} & R_M^{F,(k)} & Z_M^{F,(k)} \end{pmatrix} \tag{21}$$

where $W_i^{f,(k)} = \frac{\partial T_i^f}{\partial (\rho C)_s} |_{(\rho C)_s = (\rho C)_s^{(k)}}$, $R_i^{f,(k)} = \frac{\partial T_i^f}{\partial k_s} |_{k_s = k_s^{(k)}}$ and $Z_i^{f,(k)} = \frac{\partial T_i^f}{\partial \phi} |_{\phi = \phi^{(k)}}$ are the sensitivity coefficients and k is the number of iterations.

If we suppose that $J(p^{(k)})$ is a full rank matrix, the problem (19) has a unique solution which writes:

$$m^{(k)} = -(J(p^{(k)})^t J(p^{(k)}))^{-1} J(p^{(k)})^t r(p^{(k)}) \tag{22}$$

Algorithm. The optimization of the functional S (14) is performed by the Gauss–Newton method using the following algorithm:

1. choose an initial value $p^{(0)}$, for example $p^{(0)} = p_{\text{estimated}}$;
Loop of iterations till convergence
2. calculate $g(p^{(k)})$ by solving the state equation (1), then determine $r(p^{(k)})$;
3. calculate the Jacobian $J(p^{(k)})$;
4. solve the linear system $J(p^{(k)})^t J(p^{(k)}) m^{(k)} = -J(p^{(k)})^t r(p^{(k)})$;
5. $p^{(k+1)} = p^{(k)} + m^{(k)}$.
End of the loop

We can notice that the gradient is an essential ingredient for the method of Gauss–Newton. In the following, we present how to calculate the gradient by the sensitivity functions. Thus, we study the sensitivity of temperature field in the system of heat diffusion with respect to the unknown parameters $(\rho C)_s, k_s$ and ϕ . First of all, we differentiate the energy equation in (1) with respect to the parameter p_j

$$\frac{\partial}{\partial p_j} \left[(\rho C)_e \frac{\partial T}{\partial t} \right] = \text{div} \left(\frac{\partial}{\partial p_j} [k_e \overrightarrow{\text{grad}} T] \right) \tag{23}$$

After some mathematical manipulations, we obtain in $\Omega \times (0, t_{end}]$

$$\begin{aligned} (\rho C)_e(T) \frac{\partial U_j(x, t)}{\partial t} + \frac{d(\rho C)_e(T)}{dT} U_j(x, t) \frac{\partial T(x, t)}{\partial t} \\ = \text{div}(k_e(T) \overrightarrow{\text{grad}} U_j(x, t)) + \text{div} \left(\frac{dk_e(T)}{dT} U_j(x, t) \overrightarrow{\text{grad}} T(x, t) \right) \end{aligned} \tag{24}$$

where $U_j = \partial T / \partial p_j$.

The sensitivity model is supplemented by the initial conditions, namely

$$t = 0: \quad U_j(x, 0) = U_{j0} \quad \text{in } \Omega \tag{25}$$

If the sensitivity analysis does not concern the initial temperatures then the condition (25) is uniform (zero–one).

The boundary conditions of the equations are given by the Dirichlet boundary condition

$$U_j(x, t) = U_j^D(x, t) \quad \text{on } \Gamma^D \times (0, t_{end}] \tag{26}$$

and the Neumann boundary condition

$$U_j(x, t) \cdot \nu = U_j^N(x, t) \quad \text{on } \Gamma^N \times (0, t_{end}] \tag{27}$$

In order to determine the sensitivity coefficients appearing in the Jacobian (21), the governing energy equation in the system (1) should be differentiated with respect to $(\rho C)_s, k_s$ and ϕ respectively. For instance, in one dimension ($d = 1$), we calculate the following derivatives:

$$\begin{aligned} \frac{d(\rho C)_e}{dT} &= \phi \rho_f \frac{dC_f}{dT} + \phi C_f \frac{d\rho_f}{dT} + (1 - \phi) \\ &= \phi \rho_f \left[(C_v - C_l) \frac{d\sigma}{dT} + L \frac{d^2\sigma}{dT^2} \right] + \phi C_f (\rho_v - \rho_l) \frac{d\sigma}{dT} + (1 - \phi) \end{aligned} \tag{28}$$

and

$$\frac{dk_e}{dT} = \frac{k_s dk_f/dT (\phi k_s + (1 - \phi)k_f) - (1 - \phi) dk_f/dT k_f k_s}{(\phi k_s + (1 - \phi)k_f)^2} \tag{29}$$

with

$$\frac{dk_f}{dT} = (k_v - k_l) \frac{d\sigma}{dT}$$

Thus, to have the sensitivity equations in 1D we use (28) and (29), and we use the approximation:

$$\frac{\partial}{\partial x} \left(\frac{\partial T}{\partial x} \right) \approx \frac{(\rho C)_e}{k_e} \frac{\partial T}{\partial t} \tag{30}$$

So the following additional problems in 1D should be solved:

Differentiating with respect to $(\rho C)_s$

$$\begin{aligned} \frac{\partial W}{\partial t} + \phi \frac{\rho_f}{(\rho C)_e} \left[(C_v - C_l) \frac{d\sigma}{dT} + L \frac{d^2\sigma}{dT^2} \right] W \frac{\partial T}{\partial t} + \phi \frac{C_f}{(\rho C)_e} (\rho_v - \rho_l) \frac{d\sigma}{dT} W \frac{\partial T}{\partial t} \\ + (1 - \phi) \frac{1}{(\rho C)_e} \frac{\partial T}{\partial t} - \frac{1}{(\rho C)_e} \frac{dk_e}{dT} W \frac{\partial T}{\partial t} - \frac{1}{k_e} \frac{\partial}{\partial x} \left(k_e \frac{\partial W}{\partial x} \right) = 0 \end{aligned} \tag{31}$$

Differentiating with respect to k_s

$$\begin{aligned} \frac{\partial R}{\partial t} + \phi \frac{\rho_f}{(\rho C)_e} \left[(C_v - C_l) \frac{d\sigma}{dT} + L \frac{d^2\sigma}{dT^2} \right] R \frac{\partial T}{\partial t} + \phi \frac{C_f}{(\rho C)_e} (\rho_v - \rho_l) \frac{d\sigma}{dT} R \frac{\partial T}{\partial t} \\ - \frac{\partial}{\partial x} \left(k_e \frac{\partial R}{\partial x} \right) - \frac{k_s (k_v - k_l) \frac{d\sigma}{dT} R + k_f \frac{\partial T}{\partial t}}{(\phi k_s + (1 - \phi)k_f)^2 k_e} + \frac{k_f k_s [\phi + (1 - \phi)(k_v - k_l) \frac{d\sigma}{dT} R]}{(\phi k_s + (1 - \phi)k_f)^2 k_e} \frac{\partial T}{\partial t} = 0 \end{aligned} \tag{32}$$

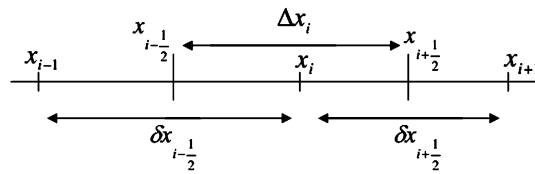


Fig. 5. Block-centered finite volume discretization of a one-dimensional problem domain.

And finally, differentiating with respect to ϕ

$$\frac{\partial Z}{\partial t} + \frac{\rho_f C_f - \rho_s C_s}{(\rho C)_e} \frac{\partial T}{\partial t} - \frac{k_f - k_s}{\phi k_s + (1 - \phi)k_f} \frac{\partial T}{\partial t} - \frac{\partial}{\partial x} \left(k_e \frac{\partial Z}{\partial x} \right) = 0 \tag{33}$$

These equations of sensitivity coefficients are completed with adequate initial and boundary conditions obtained by differentiating the initial and boundary conditions of Eq. (1) with respect to the unknown parameters. The unknowns of the sensitivity equations are W , R and Z . $(\rho C)(T)$ and $k(T)$ are dependent of the temperature T being the solution of the forward problem and not of the sensitivity coefficients, consequently, the sensitivity equations are coupled with the forward problem (1).

4. Numerical resolution

The obtained system of coupled equations (sensitivity equations + energy equation) is a nonlinear system of ordinary partial differential equations. This system has a very large size and is difficult to solve. Thus, among the large variety of existing approaches used to solve such systems, we choose the following methodology:

- (1) the use of the method of lines, where space and time discretizations are considered separately;
- (2) spatial discretization: finite volume method because it conserves mass locally and preserves the continuity of fluxes;
- (3) time discretization: Euler implicit scheme;
- (4) using a modified Newton method to deal with the present nonlinearity.

Various criteria are concerned by defining a reliable method:

- the precision of the results;
- the stability of the method;
- the computational cost;
- the facility of implementation.

In addition, a combination between these criteria must take into consideration all the difficulties present in the system (phase change interface tracking, stiff system, high nonlinearity, coupled equations, ...).

The system of Eqs. (1), (31), (32) and (33) is discretized in space using the vertex-centered finite volume method in one dimension. To apply this method we divided the computational domain into a finite volume grid or mesh (i.e., series of cells or blocks), in this case of equal width, Δx as shown in Fig. 5.

After the spatial discretization, the system of coupled equations is written as a linear system:

$$\begin{pmatrix} M(T) & 0 & 0 & 0 \\ A_W(T) & I & 0 & 0 \\ A_R(T) & 0 & I & 0 \\ A_Z(T) & 0 & 0 & I \end{pmatrix} \begin{pmatrix} \frac{dT}{dt} \\ \frac{dW}{dt} \\ \frac{dR}{dt} \\ \frac{dZ}{dt} \end{pmatrix} + \begin{pmatrix} N(T) \\ B_W(T) \\ B_R(T) \\ B_Z(T) \end{pmatrix} \begin{pmatrix} T \\ W \\ R \\ Z \end{pmatrix} = b \tag{34}$$

which is an ordinary differential equation (ODE), where the mass matrix is invertible.

In order to get a unified framework for all numerical models and methods, we introduce a matrix description of the data. Let $Y = (TW RZ)^T$, by classical transformations, the system can be written with the general form

$$\begin{cases} Y' = F(t, Y) \\ Y(t_0) = Y_0 \end{cases} \tag{35}$$

To solve this system, we propose to consider the semi-discrete model (35) and to use the framework of ODE solvers. This system can be formulated as follows

$$M_1 \frac{dY}{dt} + f_1(Y) = 0, \tag{36}$$

where

$$M_1 = \begin{pmatrix} M(T) & 0 & 0 & 0 \\ A_W(T) & I & 0 & 0 \\ A_R(T) & 0 & I & 0 \\ A_Z(T) & 0 & 0 & I \end{pmatrix} \quad \text{and} \quad f_1(Y) = \begin{pmatrix} N(T) \\ B_W(T) \\ B_R(T) \\ B_Z(T) \end{pmatrix} \begin{pmatrix} T \\ W \\ R \\ Z \end{pmatrix} - b$$

In classical global approaches, an implicit Euler scheme is used, this leads at each time step to the nonlinear system $M_1 Y + \Delta t f_1(Y) - M_1 Y_n = 0$ and the Jacobian of this system is the matrix $M_1 + \Delta t J_1$, where J_1 is the Jacobian of f_1 (these two matrices are time dependent and they are updated at each time step). This system can be solved by the Newton iterations:

$$(M_1 + \Delta t J_1)(Y^{k+1} - Y^k) = -(M_1 Y^k + \Delta t f_1(Y^k) - M_1(Y_n)) \tag{37}$$

Actually, $M_1 + \Delta t J_1$ is updated at each time step but it is independent of the iteration k .

We claim that an efficient way to solve the ODE equations is to use an ODE solver with an implicit time discretization. Our approach is a generalization of the global approach, which is a particular case with an implicit Euler scheme and a fixed time step. Thus we keep the advantage of robustness. Compared to a fixed implicit scheme such as Euler, a big advantage of ODE solvers is their control of accuracy with a variable order scheme. Moreover, these solvers provide a control of time step and the associated control of Jacobian updates (ensuring convergence of Newton iterations for example). It is in principle possible to implement these controls but they are rather sophisticated in ODE solvers and not so easy to reproduce.

In order to solve the system, we adopt the following strategy. We use software libraries and write modules clearly identified as forward problem and sensitivity equations. We apply an ODE solver (in our experiments, the `ddebd` ODE solver of the `SLATEC` library), to which we provide the temperature dependent mass matrix M , the function f , the Jacobian J and consistent initial conditions. The ODE solver applies a time discretization scheme using the BDF method (Backward Differentiation Formula) because our system is stiff and solves at each time step a system of nonlinear equations using a modified Newton method with variable time step and variable order [19,5].

On the other hand, a drawback of our approach is the large size of the linear system. However, the matrix is quite sparse and has some structure. Thus, to overcome this problem we do not reduce the size of the linear system but we provide an efficient sparse linear solver. In our experiments, we implement Newton-LU by modifying `ddebd` and by replacing the routine `dgesl` of `LAPACK` by an appropriate call in `UMFPACK` so that we can solve efficiently the large linear systems. For each iteration the linear system is solved until the assumed accuracy is achieved or after achieving the assumed value of iterations.

5. Algorithm of general resolution

The principle of resolution of inverse problem requires the estimation of the parameter p who makes the values of temperature $T(t)$, calculated by the forward problem, approach the experimental measurements $T_g(t)$.

We formulated the problem as a problem of optimization of the functional $S(p)$ defined by (14). The resolution of this problem uses the algorithm described in Section 3.2. In the implementation of the algorithm described previously, it is necessary to determine the sensitivity coefficients which represent the sensibility of the temperature field with respect to the variation of p .

The algorithm is as follows:

1. choose an initial value $p^{(0)}$
initialize the iteration $k = 0$
2. solve the system (35) (heat equation with phase change + sensitivity equations) using $p^{(k)}$ to define the parameters of the soil. The equivalent parameters of the system are calculated by the apparent heat capacity method (AHC)
 - deduce $T_i^{f,(k)}$, $W_i^{f,(k)}$, $R_i^{f,(k)}$ and $Z_i^{f,(k)}$ for $i = 1, \dots, M$ and $f = 1, \dots, F$
 - calculate the criterion $S(p^{(k)})$
3. calculate $r(p^{(k)})$ and the Jacobian $J(p^{(k)})$
solve the linear system $J(p^{(k)})^t J(p^{(k)}) m^{(k)} = -J(p^{(k)})^t r(p^{(k)})$ by the method of normal equations
4. if $S(p^{(k)}) < \epsilon$, end (the criterion of convergence must be determined)
if not, iterate: $p^{(k+1)} = p^{(k)} + m^{(k)}$
 $p^{(k)} \leftarrow p^{(k+1)}$ and go to 2.

6. Software organization

Now we have all the elements to describe the general organization of the software designed to solve the inverse problem described above in one dimension. We insist on a modular organization to guarantee the independence of the conjugate gradient calculation. We implemented a sub-program which solves the optimization problem. This sub-program calls the simulator which solves the forward problem and the sensitivity equations using the BDF solver as described above. The

Table 1
Fluid physical properties used for simulations.

Fluid phase	Heat capacity (J/kg.K)	Conductivity (W/m.K)	Density (kg/m ³)
Liquid	4000	0.6	1000
Vapor	2000	0.025	0.8

sequence of calls for the simulator is fixed by the optimization sub-program. Actually, this sub-program will be an interface between the optimizer and the subroutine of simulation which has a more complex sequence of calls. It should be mentioned that the simulator requires some informations about the geometry of the problem, the initial data, the time of simulation, the sources, etc.

The whole software uses the Fortran 90 MUESLI library (<http://www.irisa.fr/sage/edouard/canot/muesli/>) which provides linear algebra facilities using a Matlab-like syntax.

7. Example of computations

In order to validate our code, we choose a fictive example where the thermodynamic properties (volumetric heat capacity and thermal conductivity) and the porosity of the soil are constants and uniforms. These parameters are used by the forward model to calculate the temperatures at different points which are, in return, used as input data for the inverse model.

As a first approach, we choose the ideal case where the temperature measures are exacts. Using the forward problem, we obtain the values of temperature at different points of the domain and these values are considered as the experimental measures of the temperature used to validate the code of inverse problem. The physical properties of the soil used to obtain the supposed experimental values of the temperature are: $(\rho C)_s = 1.95 \times 10^6$ J/kg.K, $k_s = 0.756$ W/m.K and $\phi = 0.2\%$ (ϕ is used as the water content of the soil and not the porosity because we supposed that the porous matrix is saturated and so all the pores are saturated by water). In addition, the physical properties of the fluid used for the simulations are given in Table 1.

Figs. 6, 8 and 10 show the final results of the heat capacity, the thermal conductivity and the porosity, respectively, obtained by inverse problem after perturbing the synthetic data with a certain error coefficient as shown in Table 2. The good convergence illustrated in the curves, shows that the method of Gauss–Newton is well adapted to our problem. We have checked that the gradient is a full rank matrix, thus the problem has a unique solution.

The comparison provided in Table 2 between the numerical results and the exact values shows a good agreement. On the other hand, even if the results of the inverse problem are very close to the synthetic data, we can see a little difference due to the approximation error.

Figs. 7, 9 and 11 show that the gradient of S vanishes when the solution converges.

7.1. Influence of initial guesses

In order to study the influence of initial guesses on the convergence, we consider the previous example but with different initial guesses this time. The results of computation are shown in Table 3.

Actually, we can see that we have relatively a good convergence for the thermal conductivity and for the porosity. However, the convergence of the heat capacity seems to be far from the exact solution. This is due to the fact that the heat equation is not sensitive to the heat capacity in comparison to the other parameters. Most of time, the heat capacity converges to the initial guess as we can see in Fig. 12. Figs. 12, 13 and 14 illustrate the results shown in the previous table.

7.2. Influence of noised measures

To be close to the reality (any temperature measurement encloses inevitably some errors), we added a Gaussian noise of null average and standard deviation equal to 5°C .

Figs. 15, 17 and 19 represent the convergence of the heat capacity, the thermal conductivity and the porosity of the soil, estimated by taking into consideration the noised measures. We can see that the curves have almost the same shape as in the previous case but they converge toward different values which are not so far from those estimated without taking the noise into consideration. The gradients of the functional S with respect to the unknown parameters are illustrated in Figs. 16, 18 and 20.

8. Conclusion

This paper deals with recovering thermophysical parameters of a saturated soil (volumetric heat capacity, conductivity and porosity) based on the knowledge of temperature values at different positions in the ground. We used the least squares formulation and the Gauss–Newton method to solve an “ill-posed problem”. More precisely, in order to calculate the gradient of the cost function we used the method of sensibility analysis; this method leads to a system of three differential equations highly nonlinear numerically solved by Newton iterations. These equations are then coupled with the heat equation with

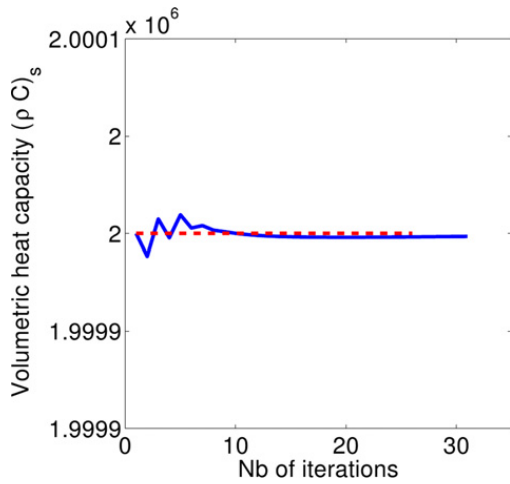


Fig. 6. Convergence of the volumetric heat capacity of the soil with respect to the number of iterations. The dashed red line represents the desired solution.

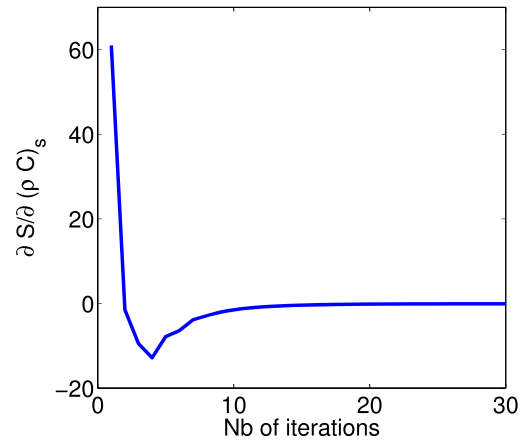


Fig. 7. Evolution of the gradient of S on $(\rho C)_s$ with respect to the number of iterations.

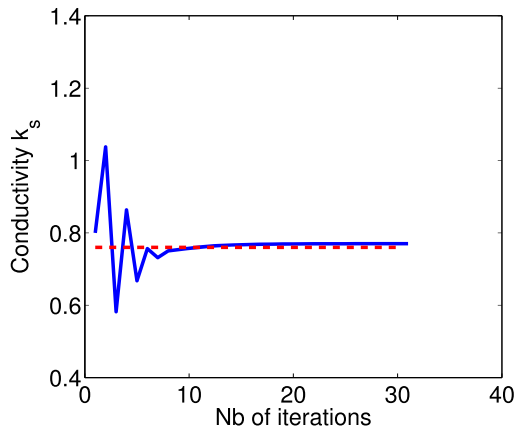


Fig. 8. Convergence of the thermal conductivity of the soil with respect to the number of iterations. The dashed red line represents the desired solution.

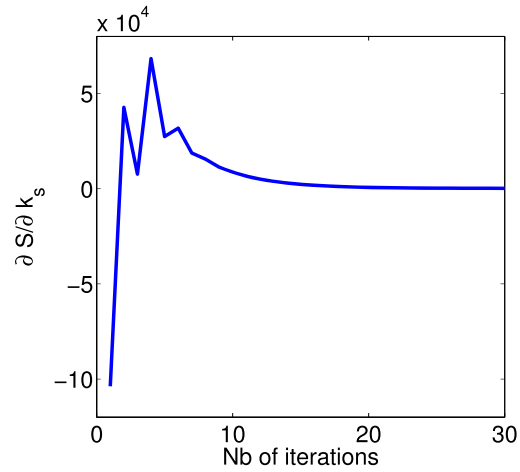


Fig. 9. Evolution of the gradient of S on k_s with respect to the number of iterations.

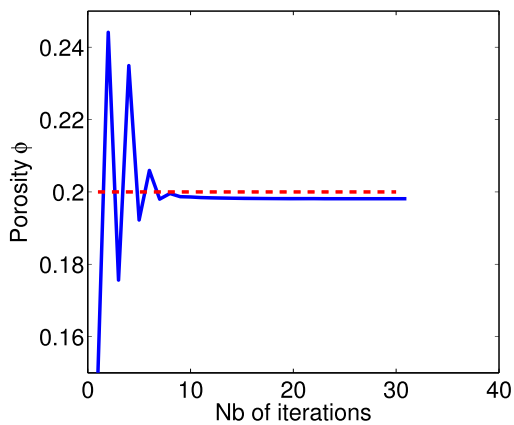


Fig. 10. Convergence of the porosity of the soil with respect to the number of iterations. The dashed red line represents the desired solution.

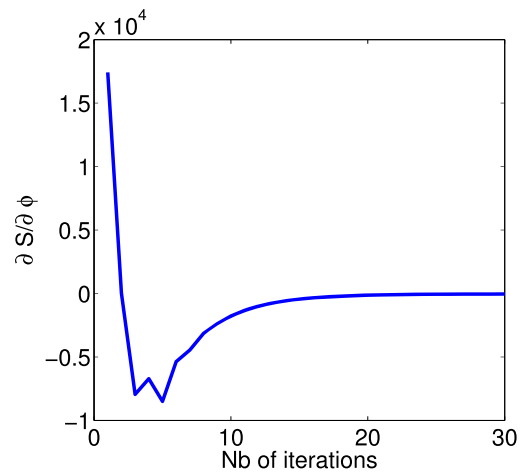


Fig. 11. Evolution of the gradient of S on ϕ with respect to the number of iterations.

Table 2
Physical properties of the soil obtained by inverse problem.

	ρC_s (J/kg.K)	k_s (W/m.K)	ϕ
Exact	1.95×10^6	0.756	0.20
Initial guess	2×10^6	0.8	0.15
Calculated	2×10^6	0.754	0.198

Table 3
Physical properties of the soil obtained by inverse problem.

	ρC_s (J/kg.K)	k_s (W/m.K)	ϕ
Exact	1.95×10^6	0.756	0.20
Initial guess	1.7×10^6	0.9	0.12
Calculated	1.699×10^6	0.69	0.209

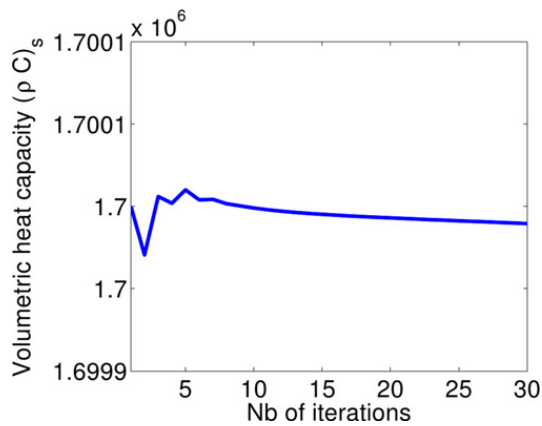


Fig. 12. Convergence of the volumetric heat capacity of the soil with respect to the number of iterations. The desired solution is 1.95×10^6 J/kg.K.

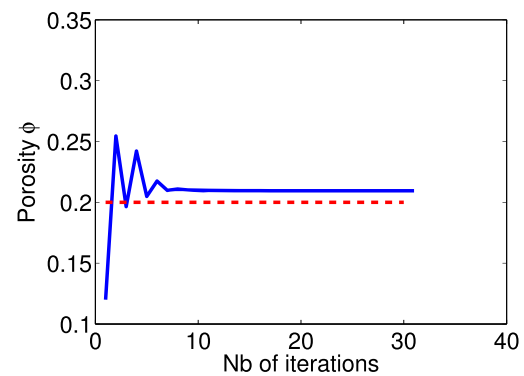


Fig. 13. Convergence of the porosity of the soil with respect to the number of iterations. The dashed red line represents the desired solution.

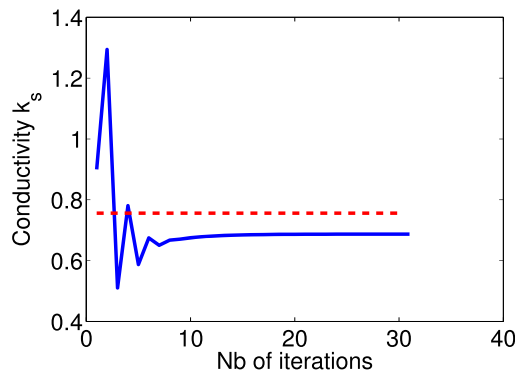


Fig. 14. Convergence of the thermal conductivity of the soil with respect to the number of iterations. The dashed red line represents the desired solution.

phase change (modeling the forward problem). Lastly, in order to numerically solve this system of coupled equations we proposed a new global approach using a BDF ODE solver.

The validation stage of our model has been performed by comparing numerical results with synthetic data obtained by the corresponding forward problem.

We must however emphasize the difficulty in recovering the original value of one physical parameter (heat capacity), because the problem is not very sensitive to this parameter; nevertheless, the obtained curves showed that the proposed algorithm is robust, produces acceptable results and converges after a few tens of iterations.

The model presented in this paper has been applied to one-dimensional configuration but it could be easily generalized to multidimensional problems.

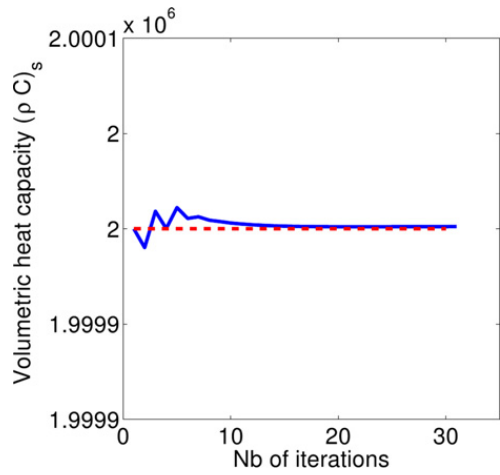


Fig. 15. Convergence of the volumetric heat capacity of the soil with respect to the number of iterations. Result obtained by the second approach taking into account the noise effect. The dashed red line represents the desired solution.

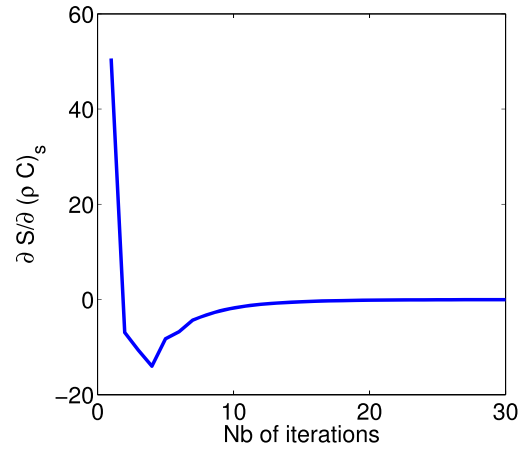


Fig. 16. Evolution of the gradient of S on $(\rho C)_s$ with respect to the number of iterations.

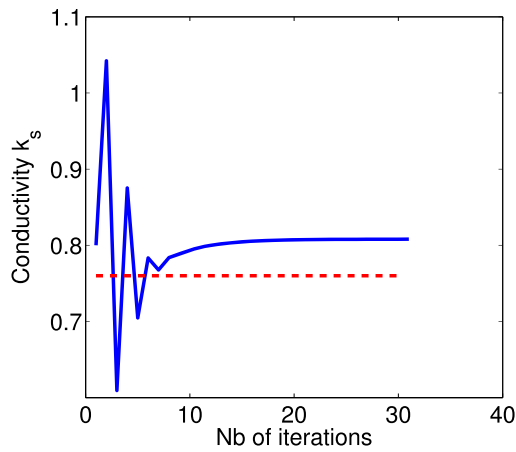


Fig. 17. Convergence of the thermal conductivity of the soil with respect to the number of iterations. Result obtained by the second approach taking into account the noise effect. The dashed red line represents the desired solution.

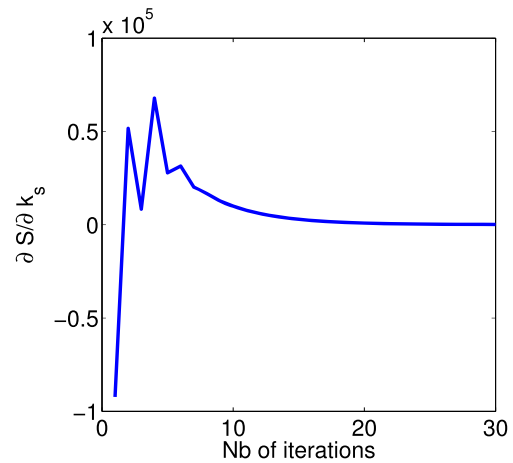


Fig. 18. Evolution of the gradient of S on k_s with respect to the number of iterations.

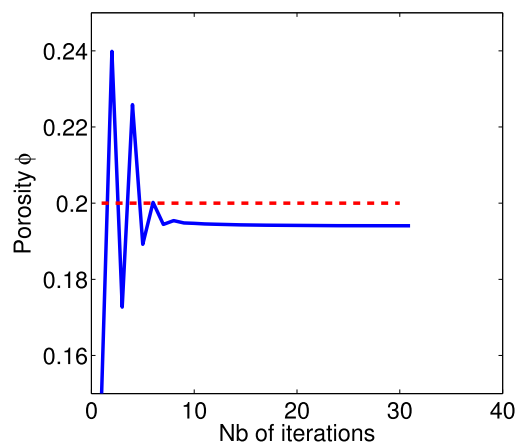


Fig. 19. Convergence of the porosity of the soil with respect to the number of iterations. Result obtained by the second approach taking into account the noise effect. The dashed red line represents the desired solution.

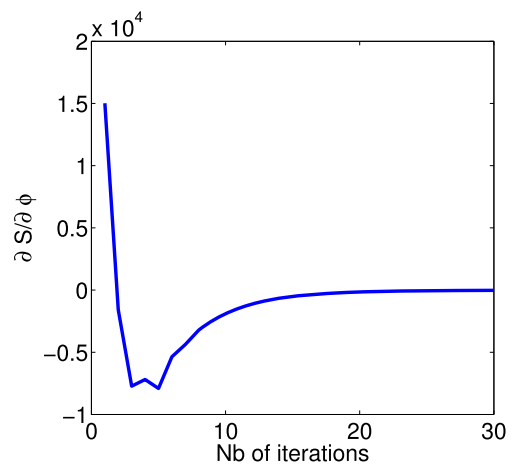


Fig. 20. Evolution of the gradient of S on ϕ with respect to the number of iterations.

References

- [1] A. Bjorck, *Numerical Methods for Least Squares Problems*, SIAM, 1990.
- [2] C. Bonacina, G. Comini, Numerical solution of phase-change problems, *International Journal of Heat Mass Transfer* 16 (1973) 1825–1832.
- [3] K.E. Brenan, S.L. Campbell, L.R. Petzold, *Numerical Solution of Initial-Value Problems in Differential-Algebraic Equations*, North-Holland, Elsevier, 1989.
- [4] F. Civan, C. M. Slipecevic, Limitation in the apparent heat capacity formulation for heat transfer with phase change, in: *Proc. Okla. Acad. Sci.*, vol. 67, 1987, pp. 83–88.
- [5] J.E. Dennis, R.B. Schnabel, *Numerical Methods for Unconstrained Optimization and Nonlinear Equations*, Prentice–Hall, Inc., New Jersey, 1983.
- [6] J.C. Ferreri, R.J. March, Using numerical models to analyze archaeological simple fires structures, in: *XIII International Congress of Prehistoric and Protohistoric Sciences, Colloquia, 5. The Lower and Middle Paleolithic Colloquium*, Forli, Italy, 8/14 September 1996, pp. 57–63.
- [7] J. Hadamard, *Lectures on Cauchy's Problem in Linear Partial Differential Equations*, Yale University Press, 1923.
- [8] S. Kim, M.C. Kim, K.Y. Kim, An integral approach to the inverse estimation of temperature-dependent thermal conductivity without internal measurements, *Computational Geosciences* 29 (1) (2002) 107–113.
- [9] P.K. Kitaniadis, *Quasi-Linear Geostatistical Theory for Inversing*, 31st ed., Water Resources Research, 1995.
- [10] J. Lukovikova, P. Matiasovsky, M. Balzovjeh, Nonlinear problem of inverse determination of heat coefficient, *Tech. Rep.*, Faculty of Civil Engineering, STU, Bratislava, Slovakia, 2004.
- [11] E. Majchrzak, M. Dziewonski, G. Katuza, Identification of cast steel latent heat by means of gradient method, *International Journal of Computational Materials Science and Surface Engineering* 1 (5) (2007) 555–570.
- [12] E. Majchrzak, J. Mendakiewicz, A.P. Belkhat, Algorithm of the mould thermal parameters identification in the system casting–mould–environment, *Journal of Materials Processing Technology* 164–165 (2005) 1544–1549.
- [13] E. Majchrzak, B. Mochnaki, J.S. Suchy, Identification of substitute thermal capacity of solidifying alloy, *Journal of Theoretical and Applied Mechanics* 46 (2) (2008) 257–268.
- [14] M.M. Mejias, H.R.B. Orlande, A comparison of different parameter estimation techniques for the identification of thermal conductivity components of orthotropic solids, in: *3rd International Conference on Inverse Problems in Engineering*, Port, Ludlow, WA, USA, 1999.
- [15] M. Muhieddine, *Simulation numérique des structures de combustion préhistoriques*, Rennes, France, 2009.
- [16] M. Muhieddine, E. Canot, R. March, Simulation of heat transfer with phase change in 3d saturated porous media, in: *3rd International Conference on Approximation Methods and Numerical Modeling in Environment and Natural Resources, Mamern09*, vol. 2, Pau, France, 2009, pp. 701–706.
- [17] M. Muhieddine, E. Canot, R. March, Various approaches for solving problems in heat conduction with phase change, *International Journal on Finite Volumes* 6 (1) (2009) 1–20.
- [18] M. Muhieddine, E. Canot, R. March, R. Delannay, Coupling heat conduction and water steam flow in a saturated porous medium, *International Journal for Numerical Methods in Engineering* 85 (2011) 1390–1414.
- [19] J.M. Ortega, W.C. Rheinboldt, *Iterative Solution of Nonlinear Equations in Several Variables*, Academic Press, 1970.
- [20] S.S. Symes, M. Kern, Inversion of reflection seismograms by differential semblance analysis: Algorithm structure and synthetic examples, *Geophysical Prospecting* 42 (1994) 565–614.
- [21] J. Wang, N. Zabarar, A Bayesian inference approach to the inverse heat conduction problem, *International Journal of Heat and Mass Transfer* 47 (2004) 3927–3941.